Available online at www.sciencedirect.com
ScienceDirect
Journal of Molecular Catalysis A: Chemical 273 (2007) 160–168
JOURNAL OF MOLECULAR CATALYSIS A: CHEMICAL
www.elsevier.com/locate/molcata

Selective hydrogenation of bromonitrobenzenes over Pt/γ-Fe_2O_3

Xiaodong Wang, Minghui Liang, Hongquan Liu, Yuan Wang *

Beijing National Laboratory for Molecular Sciences, State Key Laboratory for Structural Chemistry of Unstable and Stable Species, College of Chemistry & Molecular Engineering, Peking University, Beijing 100871, PR China

Received 20 January 2007; received in revised form 3 April 2007; accepted 3 April 2007
Available online 7 April 2007

Abstract

The Pt/γ-Fe_2O_3 nanocomposite catalyst exhibited high catalytic activities and superior selectivities to *ortho*-bromoaniline (*o*-BAN), *meta*-bromoaniline (*m*-BAN) and *para*-bromoaniline (*p*-BAN) in the hydrogenation of *ortho*-bromonitrobenzene (*o*-BNB), *meta*-bromonitrobenzene (*m*-BNB) and *para*-bromonitrobenzene (*p*-BNB), respectively. The hydrodebromination of bromoanilines (BANs) over the Pt/γ-Fe_2O_3 nanocomposite catalyst was fully suppressed even at complete conversion of the substrates for the first time. Elevating hydrogen pressure from 0.1 to 2.0 MPa could not only increase the hydrogenation rates of *o*-BNB, *m*-BNB and *p*-BNB by 8.8, 11.8 and 10.0 times, respectively, but also further improve the selectivities to *o*-BAN, *m*-BAN and *p*-BAN to a level higher than 99.9%. A new hydrodebromination pathway in the hydrogenation of bromonitrobenzenes (BNBs), i.e. through the hydrodebromination of the condensation intermediates was revealed.

Keywords: Platinum nanocomposite catalyst; Bromonitrobenzene; Bromoaniline; Hydrogenation; Hydrodebromination

1. Introduction

Aromatic haloamines are important organic intermediates in the synthesis chemistry of organic dyes, perfumes, herbicides, pesticides, preservatives, plant growth regulators, medicines and light sensitive or nonlinear optical materials [1,2]. These widely applied organic amines are currently produced mainly through selective hydrogenation of the corresponding aromatic halonitro compounds over transition metal catalysts, such as noble metals and Raney nickel. However, over usual metal catalysts, it is difficult to completely avoid the hydrodehalogenation of the aromatic haloamines in the hydrogenation of aromatic halonitro compounds to aromatic haloamines, because hydrogenolysis of the carbon–halogen bond is enhanced by amino substitution in the aromatic ring [3]. Dehalogenation has been shown to occur over the catalysts of platinum, palladium, rhodium, nickel and copper chromite, etc.

Metal nanoclusters have proved to be promising building blocks for assembling novel heterogeneous catalysts. Recently, we reported that Ru/SnO_2 [4] and Pt/γ-Fe_2O_3 [5] nanocomposite catalysts exhibited excellent catalytic activities and selectivity for the selective hydrogenation of *ortho*-chloronitrobenzene (*o*-CNB). Over the magnetic Pt/γ-Fe_2O_3 nanocomposite catalyst, the hydrodechlorination of *ortho*-chloroaniline (*o*-CAN) was completely inhibited, and the turnover number for the hydrogenation of *o*-CBN to *o*-CAN could achieve more than 100,000. The magnetic nanocomposite catalyst could be recovered from the reaction system in an applied magnetic field.

Compared with chloroanilines (CANs), bromoanilines (BANs) are more convenient intermediates for the syntheses of functional molecules and materials due to the ease of Br–C bond activation. BANs are important precursors for synthesizing a variety of biologically and pharmacologically active compounds, such as quinazoline [6], spiropiperidine [7], substituted pyrrolopyrimidine [8], pyridazino-annelated ring system [9] and benzo-β-carboline isoneocryptolepine [10]. These substances can be used for antifungal, antitumor and antihypertensive agents, neurokinin, oxytocin and bradykinin antagonists, or medicine for malaria [6–10]. In addition, BANs are versatile intermediates in the syntheses of conducting polymers [11,12] and organometallic compounds [13].

Considerable attention has been attracted to chloronitrobenzenes (CNBs) hydrogenation [14–21], whereas much less effort has been paid to the selective hydrogenation of bromonitrobenzenes (BNBs) for producing the corresponding BANs, partly due to the difficulty to suppress the hydrodebromination reac-

* Corresponding author. Tel.: +86 10 6275 7497; fax: +86 10 6276 5769.
E-mail address: wangy@pku.edu.cn (Y. Wang).

1381-1169/$ – see front matter © 2007 Elsevier B.V. All rights reserved.
doi:10.1016/j.molcata.2007.04.004

tion, since the Br–C bond is more susceptible to hydrogenolysis than the Cl–C bond [3,22–24]. William investigated the effects of solvent and hydrogen pressure on the catalytic properties of commercially available Pt/C, Pt/C-sulfided, Rh/C and Raney Ni catalysts for BNBs hydrogenation. The best yields of *o*-BAN, *m*-BAN and *p*-BAN over these catalysts were not more than 84, 96 and 93 mol%, respectively [24]. The selective hydrogenation of BNBs to BANs is an ideal model reaction for the investigation aiming at suppressing the hydrodehalogenation processes in the hydrogenation of aromatic halonitro compounds. Moreover, improving the selectivity to some BANs in the hydrogenation of corresponding BNBs such as *m*-BNB is of high economic value.

The previous strategies for minimizing hydrodebromination in BNBs hydrogenation were either applying partly poisoned catalysts or introducing debromination inhibitors into the reaction media. For example, when phosphorous acid was used as an inhibitor for reducing the debromination in the hydrogenation of *p*-BNB over a Pt/C catalyst, the debromination product was reported to be 1.6 mol% [23]. By these means, the selectivity to BANs could be improved obviously, but the hydrodebromination process of BANs could not be fully suppressed and the hydrogenation rates of BNBs were usually restrained synchronously [22–24].

It is still a challenge to completely inhibit the hydrodebromination of BANs and produce BANs of high purity by highly efficient hydrogenation of BNBs. In this paper, we report the excellent catalytic properties of our Pt/γ-Fe_2O_3 nanocomposite [5] for the selective hydrogenation of BNBs. Over this catalyst, the reactions of interest can accomplish with high rates and superior selectivities to BANs (>99.9%), and the hydrodebromination of BANs was fully suppressed for the first time. A new hydrodebromination route was revealed, and the effect of hydrogen pressure on the catalytic properties was examined.

2. Experimental

2.1. Reagents

Hydrogen (99.999%) was supplied by Beijing Gases Company. Pt/C (5 wt.%) was purchased from Acros. *o*-BNB (Alfa, 99%), *m*-BNB (Acros, 99%) and *p*-BNB (Alfa, 98%) were recrystallized in methanol. *o*-BAN (Aldrich, 98%), *m*-BAN (Alfa, 98%), *p*-BAN (Alfa, >98%) and methanol (Fisher, HPLC grade, 99.9%) were used without further purification. Other reagents used in this work were analytical grade.

2.2. Catalyst preparation

The Pt/γ-Fe_2O_3 nanocomposite was prepared by the method reported recently [5]. In a typical experiment, an ethylene glycol colloidal solution of Pt nanoclusters (stabilized with ethylene glycol and simple ions) [25] and a sol of ferric hydroxide were mixed at the required ratio. The obtained mixture was heated in a teflonlined autoclave at 353 K for 3 days, producing a magnetic precipitate (Pt/γ-Fe_3O_4). After separated in a magnetic field, the precipitate was dried and oxidized at 353 K to give a brownish red Pt/γ-Fe_2O_3 nanocomposite catalyst.

2.3. Catalytic reactions

Hydrogenation of BNBs was carried out in a 50-ml reactor with magnetic stirring at 303 K and atmospheric pressure. Prior to the reaction, air in the system was replaced by hydrogen 15 times. 0.05 g of Pt/γ-Fe_2O_3 (1 wt.%) or 0.01 g of Pt/C (5 wt.%), dispersed in 5 ml of methanol, was activated under hydrogen for 30 min, then 10 ml methanol solution of *o*-BNB, *m*-BNB or *p*-BNB (0.075 M) was added into the reactor to start the reaction. The hydrogen uptake was monitored by a constant pressure gas burette. The products were identified by GC–MS coupling (Perkin-XL) or organic mass spectrometry (ZAB-HS), and analyzed by gas chromatography (Shimadzu, GC-2010), equipped with a FID detector and a capillary column Rtx-5MS (Ø 0.25 mm × 60 m). Biphenyl as an internal standard was added into the samples for GC measurements rather than the reaction system to avoid its influence on the hydrogenation reactions. The semi-quantitative analysis of trace aniline (AN) in the reaction mixture was conducted by comparing the AN peak area in GC with those of standard solutions with ratios of AN to BAN less than 0.1%.

3. Results and discussion

The Pt/γ-Fe_2O_3 (1 wt.%) magnetic nanocomposite used in this work has been well characterized in the previous work [5]. The catalyst's specific surface area is 22 m^2/g and the Pt nanoclusters, average particle size in 2.6 nm as measured by scanning transmission electron microscope (STEM), are well dispersed in the matrix composed of γ-Fe_2O_3 nanoparticles.

Fig. 1 shows the cumulative hydrogen uptake curves in the hydrogenation of *o*-BNB over the Pt/γ-Fe_2O_3 and Pt/C catalysts. Over the Pt/γ-Fe_2O_3 nanocomposite catalyst, the hydrogen uptake reached the theoretic amount for *o*-BAN formation within 28 min. Subsequently, no more increase in the hydrogen uptake was detected within extended reaction time. Quite different features of the hydrogen uptake curves were observed over the Pt/C

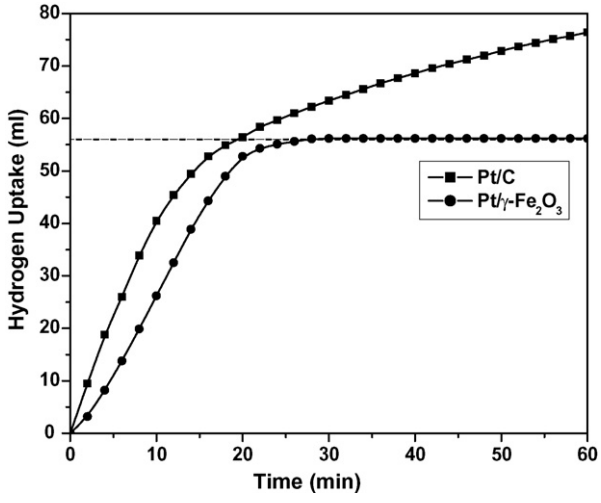

Fig. 1. Cumulative hydrogen uptake of *o*-BNB hydrogenation over Pt/γ-Fe_2O_3 and Pt/C catalysts. *Reaction conditions*: temperature, 303 K; hydrogen pressure, 0.1 MPa; loading of Pt, 0.5 mg; solvent, 15 ml methanol; substrate, 0.75 mmol.

Table 1
Catalytic properties of Pt/γ-Fe_2O_3 and Pt/C catalysts for the hydrogenation of *o*-BNB[a]

Catalyst	Loading of Pt (mg)	P_H[b] (MPa)	Reaction time	Reaction rate[c]	Selectivity (mol%)	
					o-BAN	AN
Pt/C[d]	0.5	0.1	16 min		50	11
Pt/C	0.5	0.1	60 min	0.081	29	63
Pt/C	0.5	0.1	4 h		0	91
Pt/γ-Fe_2O_3	0.5	0.1	28 min	0.174	>99.7	0.2
Pt/γ-Fe_2O_3	0.5	0.1	5 h		>99.7	0.2
Pt/γ-Fe_2O_3	0.1	1.0	21 min	1.161	>99.9	<0.1
Pt/γ-Fe_2O_3	0.1	1.0	5 h		>99.9	<0.1
Pt/γ-Fe_2O_3	0.1	2.0	16 min	1.524	>99.9	<0.1
Pt/γ-Fe_2O_3	0.1	2.0	5 h		>99.9	<0.1

[a] *Reaction conditions*: temperature, 303 K; solvent, 15 ml methanol; substrate, 0.75 mmol.
[b] Hydrogen pressure.
[c] Average rate, $mol_{o\text{-BNB}}/(mol_{Pt}\ s)$, calculated based on the amount of catalysts and the required time for exhausting *o*-BNB and all intermediates.
[d] The reaction was not complete.

catalyst, which were characterized by a fast initial rate of hydrogen consumption and a further increase in hydrogen uptake after the theoretic amount of hydrogen for *o*-BAN formation was consumed. The kinetic curves for the hydrogenation of *m*-BNB and *p*-BNB over the Pt/γ-Fe_2O_3 and Pt/C catalysts, respectively, were quite similar to those for *o*-BNB hydrogenation over these catalysts as shown in Fig. 1.

The results for *o*-BNB hydrogenation over the Pt/γ-Fe_2O_3 and Pt/C catalysts are summarized in Table 1. It can be seen that the Pt/C catalyst exhibited a poor selectivity and a low catalytic activity for the formation of the object product, *o*-BAN. Over the Pt/C catalyst, the average reaction rate was 0.081 $mol_{o\text{-BNB}}/(mol_{Pt}\ s)$ at the given conditions and the selectivities to *o*-BAN and AN at the time when reaction completed were 29 and 63%, respectively, as measured by GC. The highest yield of *o*-BAN obtained over the Pt/C catalyst was only 50% during the whole reaction course. When extending the reaction time to 4 h, the desired product, *o*-BAN, was wholly exhausted over the Pt/C catalyst and transformed to 91% of AN as well as 9% of other byproducts.

Excellent catalytic properties were obtained over the Pt/γ-Fe_2O_3 nanocomposite catalyst. Over this catalyst, the average *o*-BAN formation rate, 0.174 $mol_{o\text{-BAN}}/(mol_{Pt}\ s)$, at 303 K and 0.1 MPa of hydrogen pressure was more than twofold higher than that over the Pt/C catalyst, and an *o*-BAN selectivity of 99.7% could be easily obtained. The content of AN in the final products was only about 0.2% (the analysis method was detailed in Section 2.3). Though the reaction was complete within 28 min, it was found that extending the reaction time to 5 h did not cause detectable decrease in the catalytic selectivity. Moreover, the hydrogenation rate of *o*-BNB over the Pt/γ-Fe_2O_3 catalyst could be elevated by 6.7 and 8.8 times by increasing hydrogen pressure from 0.1 to 1.0 and 2.0 MPa, respectively. Simultaneously, the selectivity to *o*-BAN could be further improved at the elevated hydrogen pressure to a level higher than 99.9% that could be maintained even when the reaction time was extended after the exhaustion of the substrate.

In the case of *m*-BNB and *p*-BNB hydrogenation, the highest yield of *m*-BAN and *p*-BAN obtained over the Pt/C catalyst was 79 and 66%, respectively. However, when the reaction was complete, represented by the substrate and all intermediates disappeared, the yield of *m*-BAN and *p*-BAN over the Pt/C catalyst descended to 75 and 38%, respectively. Sequentially extending the reaction time would cause further debromination of *m*-BAN and *p*-BAN over the Pt/C catalyst as shown in Tables 2 and 3.

Table 2
Catalytic properties of Pt/γ-Fe_2O_3 and Pt/C catalysts for the hydrogenation of *m*-BNB[a]

Catalyst	Loading of Pt (mg)	P_H (MPa)	Reaction time	Reaction rate[b]	Selectivity (mol%)	
					m-BAN	AN
Pt/C[c]	0.5	0.1	25 min		79	11
Pt/C	0.5	0.1	40 min	0.122	75	19
Pt/C	0.5	0.1	5 h		27	64
Pt/γ-Fe_2O_3	0.5	0.1	26 min	0.188	>99.8	0.1
Pt/γ-Fe_2O_3	0.5	0.1	5 h		>99.8	0.1
Pt/γ-Fe_2O_3	0.1	1.0	15 min	1.626	>99.9	<0.1
Pt/γ-Fe_2O_3	0.1	1.0	5 h		>99.9	<0.1
Pt/γ-Fe_2O_3	0.1	2.0	11 min	2.217	>99.9	<0.1
Pt/γ-Fe_2O_3	0.1	2.0	5 h		>99.9	<0.1

[a] Reaction conditions are similar to those in Table 1.
[b] Average rate, $mol_{m\text{-BNB}}/(mol_{Pt}\ s)$.
[c] The reaction was not complete.

Table 3
Catalytic properties of Pt/γ-Fe_2O_3 and Pt/C catalysts for the hydrogenation of *p*-BNB[a]

Catalyst	Loading of Pt (mg)	P_H (MPa)	Reaction time	Reaction rate[b]	Selectivity (mol%)	
					p-BAN	AN
Pt/C[c]	0.5	0.1	8 min		66	8
Pt/C	0.5	0.1	25 min	0.195	38	55
Pt/C	0.5	0.1	4.5 h		0	92
Pt/γ-Fe_2O_3	0.5	0.1	24 min	0.203	>99.8	0.1
Pt/γ-Fe_2O_3	0.5	0.1	5 h		>99.8	0.1
Pt/γ-Fe_2O_3	0.1	1.0	17 min	1.434	>99.9	<0.1
Pt/γ-Fe_2O_3	0.1	1.0	5 h		>99.9	<0.1
Pt/γ-Fe_2O_3	0.1	2.0	12 min	2.032	>99.9	<0.1
Pt/γ-Fe_2O_3	0.1	2.0	5 h		>99.9	<0.1

[a] Reaction conditions are similar to those in Table 1.
[b] Average rate, $mol_{p\text{-BNB}}/(mol_{Pt}\ s)$.
[c] The reaction was not complete.

On the contrary, over the Pt/γ-Fe_2O_3 catalyst, the high selectivity to *m*-BAN and *p*-BAN of about 99.8%, obtained at 26 and 24 min when the hydrogenation of *m*-BNB and *p*-BNB was fully accomplished, respectively, could be maintained even after the reaction time was extended to 5 h. Similar to the case of *o*-BNB hydrogenation over Pt/γ-Fe_2O_3, elevating hydrogen pressure from 0.1 to 1.0 and 2.0 MPa could increase the reaction rate by 8.6 and 11.8 times for *m*-BNB hydrogenation, and by 7.1 and 10.0 times for *p*-BNB hydrogenation, respectively. Furthermore, the selectivity to *m*-BAN and *p*-BAN, over 99.9%, could be maintained under such high hydrogen pressure in the presence of the Pt/γ-Fe_2O_3 catalyst, and no loss of the superior selectivity was detected within 5 h.

To validate the inhibiting ability of iron oxide in the Pt/γ-Fe_2O_3 nanocomposite catalyst for BANs debromination, we carried out the hydrogenolysis experiment of the hydrogenation product, *p*-BAN, over the Pt/γ-Fe_2O_3 and Pt/C catalysts. As listed in Table 4, no AN was detected over the activated Pt/γ-Fe_2O_3 catalyst during the long reaction period of 5 h, which further confirmed that the hydrodebromination of BANs was fully suppressed over the Pt/γ-Fe_2O_3 catalyst. In contrast, over the activated Pt/C catalyst, obvious hydrodebromination was observed. When the hydrogenolysis of *p*-BAN was conducted for 5 h in the given experimental conditions, 90% of AN was produced and only 2% of *p*-BAN remained.

The preceding results suggest that the Pt/γ-Fe_2O_3 nanocomposite is a promising catalyst for effectively producing BANs with high purity. On the other hand, since the hydrodebromination of BANs was completely suppressed over the Pt/γ-Fe_2O_3 catalyst, it can be certainly concluded that the trace of AN present in the hydrogenation products was derived from other debromination route.

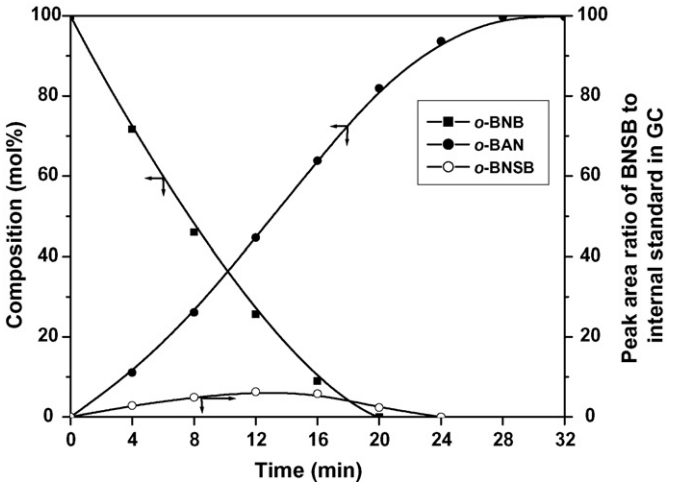

Fig. 2. Composition of the reaction mixture of *o*-BNB hydrogenation over the Pt/γ-Fe_2O_3 catalyst as a function of time. *Reaction conditions*: temperature, 303 K; hydrogen pressure, 0.1 MPa; loading of Pt, 0.5 mg; solvent, 15 ml methanol; substrate, 0.75 mmol. Biphenyl with a concentration of 0.03 g/l in methanol was used as the internal standard for quantitative analysis of the samples by GC measurements.

The widely accepted reaction pathways for the hydrogenation of halonitrobenzenes are shown in Scheme 1 [26,27], in which there are two main routes. One (**I**) is the direct reduction of nitro group in halonitrobenzenes (**1**), through the nitroso- (**2**) and hydroxylamine- (**3**) intermediates to the haloaniline (**4**) products

Table 4
Hydrodebromination of *p*-BAN over Pt/γ-Fe_2O_3 and Pt/C catalysts[a]

Catalyst	Loading of Pt (mg)	P_H (MPa)	Reaction time (h)	Reaction rate[b]	Composition (mol%)	
					p-BAN	AN
Pt/C	0.5	0.1	5	0.015	2	90
Pt/γ-Fe_2O_3	0.5	0.1	5	–	> 99.9	<0.1

[a] Reaction conditions: temperature, 303 K; solvent, 15 ml methanol; *p*-BAN, 0.75 mmol.
[b] Average rate, $mol_{AN}/(mol_{Pt}\ s)$, calculated based on the amount of the catalysts and formed AN within the reaction time.

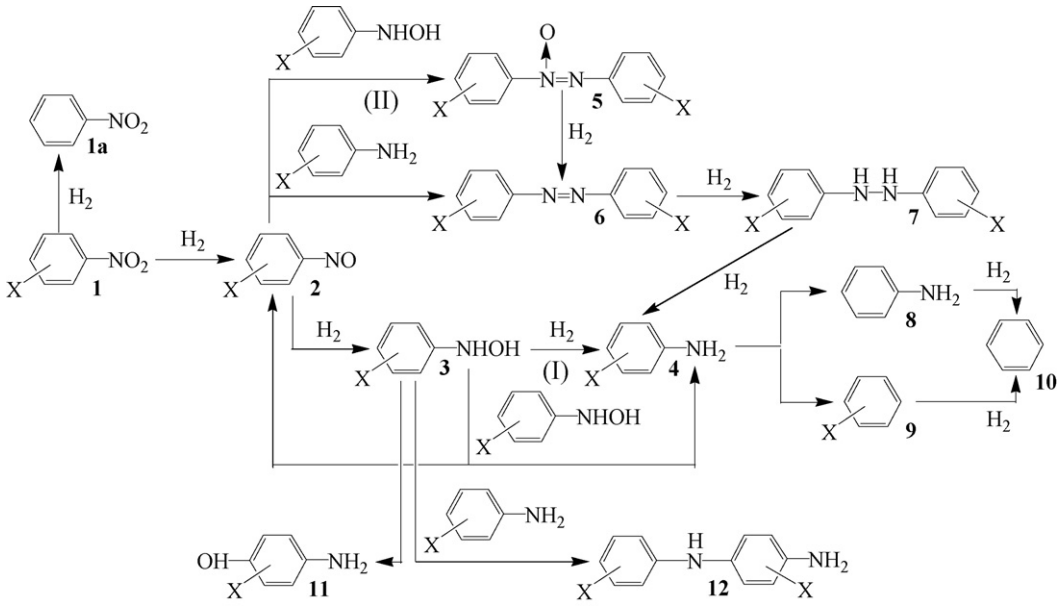

Scheme 1. Widely accepted reaction pathways related to the hydrogenation of halonitrobenzenes.

[28–31]. The other (**II**) is the condensation of the nitroso- (**2**) and hydroxylamine- (**3**) intermediates to form azoxy- (**5**) intermediates, followed by the hydrogenation through the azo- (**6**) and hydrazo- (**7**) intermediates to the desired haloaniline (**4**) products [31,32]. Haloanilines were thought to be the most susceptive compounds to the catalytic hydrogenolysis over usual metal catalysts, resulting in the cleavages of the carbon–halogen bond, carbon–nitrogen bond, or both to form aniline (**8**), halobenzenes (**9**), or benzene (**10**) [30–33]. Besides, the formation of aminohalophenol (**11**) byproducts can be driven by the Bamberger's rearrangement of *N*-phenylhydroxylamines (**3**) [34,35] in a strong acidic medium, e.g. sulphuric acid. Under proper acidic conditions, the reaction of hydroxylamines (**3**) with haloanilines (**4**) yielding amino-(*N*,*N*′-dihalophenyl)amines (**12**) can proceed [28,36].

In the present experiments of *o*-BNB, *m*-BNB and *p*-BNB hydrogenation, we observed the formations, increases followed by the decreases in amount, as well as the disappearances of *o*-bromonitrosobenzene (*o*-BNSB), *m*-bromonitrosobenzene (*m*-BNSB) and *p*-bromonitrosobenzene (*p*-BNSB) intermediates (**2**) over both Pt/γ-Fe_2O_3 and Pt/C catalysts (Figs. 2–7). It was reported that the hydroxylamine- (**3**) intermediates would decompose to nitroso- (**2**) compounds during GC analysis [37,38]. Probably, bromophenylhydroxylamines (BPHs) (**3**) are the prevailing intermediates present in the reaction media. Besides, by mass spectrometry analysis, we ascertained the formation of dibromoazoxybenzenes (**5**), dibromoazobenzenes (**6**) and dibromohydrazobenzenes (**7**) in the reaction course over the Pt/γ-Fe_2O_3 and Pt/C catalysts. These results indicated that the hydrogenation of BNBs over both catalysts follows two parallel routes, **I** and **II**, simultaneously. The further increase in *o*-BAN, *m*-BAN and *p*-BAN yields over the Pt/γ-Fe_2O_3 catalyst after the exhaustion of BNSB intermediates should be derived from the hydrogenation of the condensation intermediates (Figs. 2, 4 and 6).

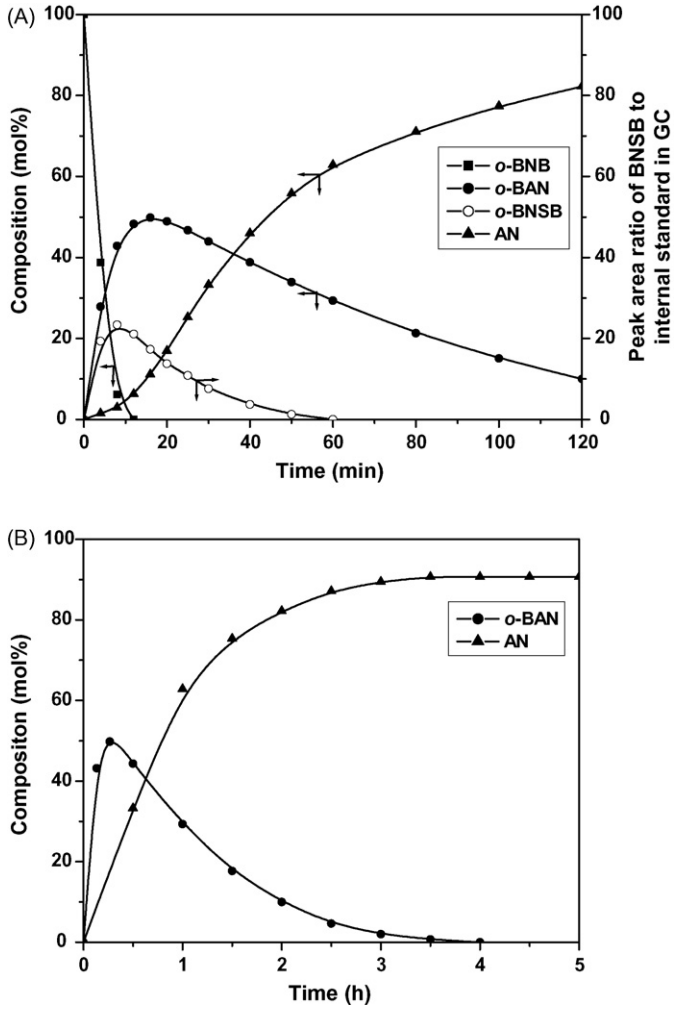

Fig. 3. Composition of the reaction mixture of *o*-BNB hydrogenation over the Pt/C catalyst at different time scales. (A) From the start to 120 min; (B) from the start to 5 h. Reaction conditions are similar to those in Fig. 2.

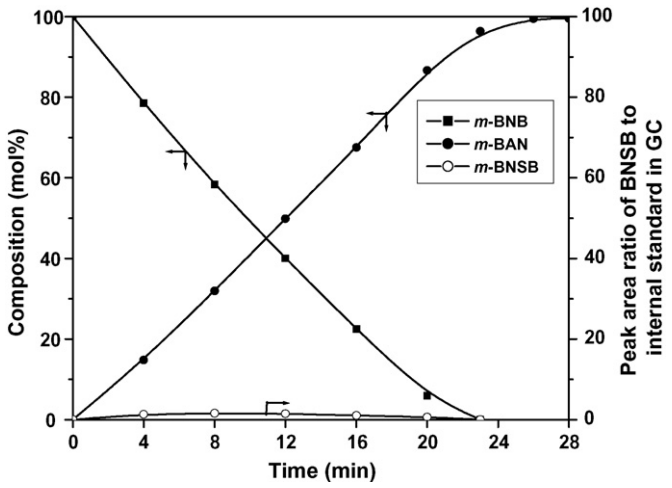

Fig. 4. Composition of the reaction mixture of *m*-BNB hydrogenation over the Pt/γ-Fe_2O_3 catalyst as a function of time. Reaction conditions are similar to those in Fig. 2.

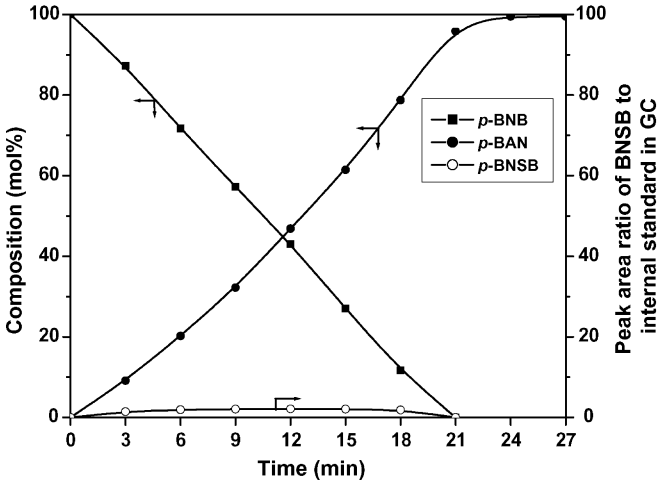

Fig. 6. Composition of the reaction mixture of *p*-BNB hydrogenation over the Pt/γ-Fe_2O_3 catalyst as a function of time. Reaction conditions are similar to those in Fig. 2.

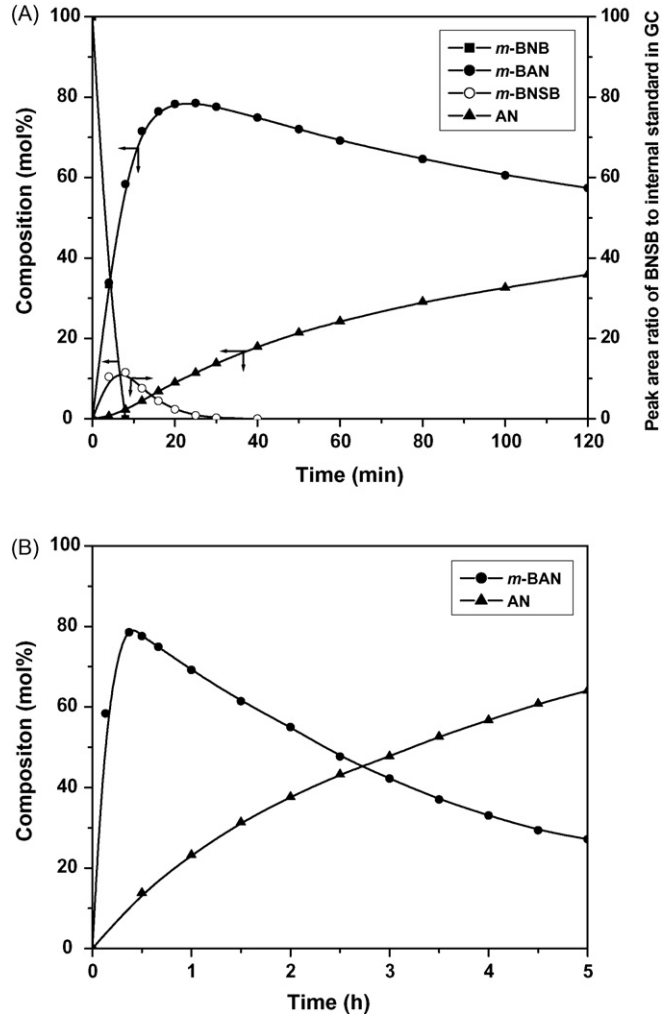

Fig. 5. Composition of the reaction mixture of *m*-BNB hydrogenation over the Pt/C catalyst at different time scales. (A) From the start to 120 min; (B) from the start to 5 h. Reaction conditions are similar to those in Fig. 2.

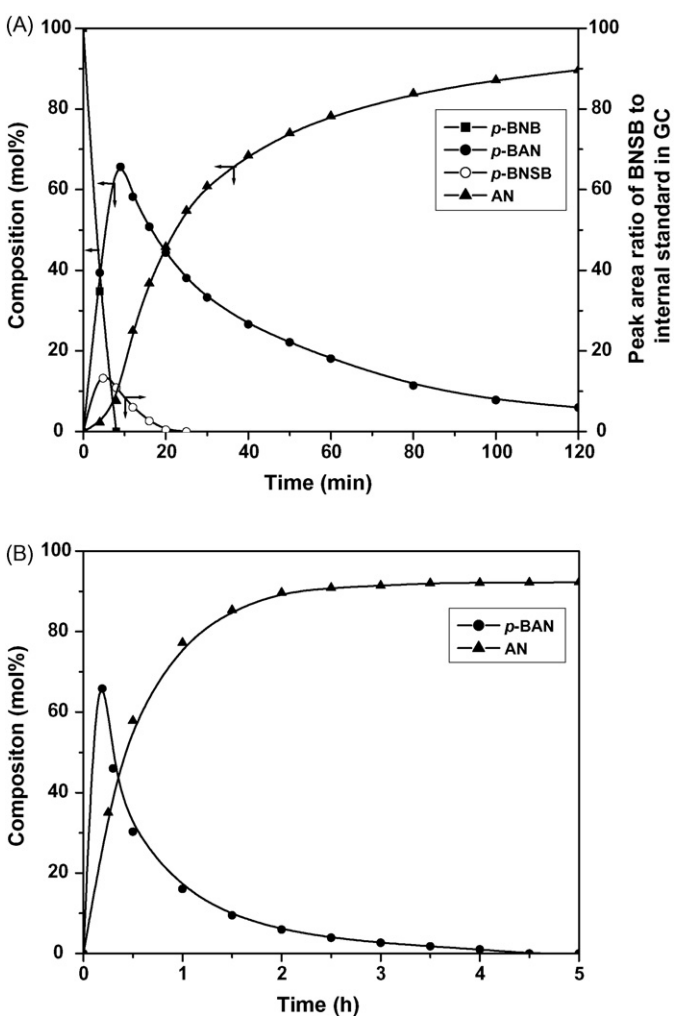

Fig. 7. Composition of the reaction mixture of *p*-BNB hydrogenation over the Pt/C catalyst at different time scales. (A) From the start to 120 min; (B) from the start to 5 h. Reaction conditions are similar to those in Fig. 2.

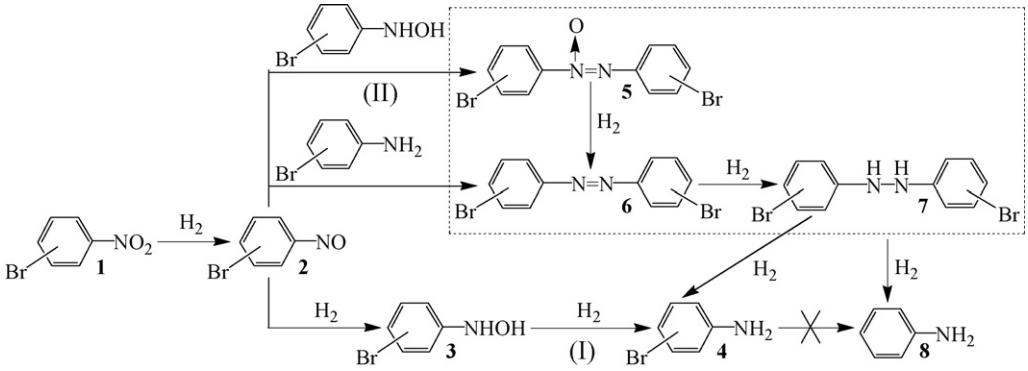

Scheme 2. Reaction pathways related to the hydrogenation of BNBs over the Pt/γ-Fe_2O_3 catalyst.

Pascoe [24] reported that disproportionation of the BPH intermediates (**3**) to BNSB compounds (**2**) and BAN products (**4**) would not occur at low reaction temperature due to the absence of enough energy. On the other hand, he did not detect any debrominated intermediate in the hydrogenation of BNBs over the Pt/C, Pt/C-sulfided, Rh/C and Raney Ni catalysts, thereby pointed out that debromination occurred only to the BAN products over the tested catalysts.

However, as mentioned above, the hydrodebromination of the BAN products over the Pt/γ-Fe_2O_3 catalyst was completely suppressed, and the trace of AN formed only before the desired reactions were complete. To ascertain the new debromination pathway, we investigated the hydrogenation of *4*,*4′*-dibromoazoxybenzene (**5**) over the Pt/γ-Fe_2O_3 catalyst and found that AN, as the unique byproduct with a selectivity of about 0.4%, produced beside the main product of *p*-BAN. These results suggested that the trace of AN (Table 3) present in the products of *p*-BNB hydrogenation over the Pt/γ-Fe_2O_3 catalyst was derived from pathway **II**, i.e., produced through the hydrodebromination of the condensation intermediates (**5**-**7**), since no debrominated byproduct directly coming from the substrates or pathway **I** was detected in *p*-BNB hydrogenation over this catalyst. To the best of our knowledge, the dehalogenation pathway through the condensation intermediates in halonitrobenzenes hydrogenation has not yet been reported due to the difficulty in clearly distinguishing the dehalogenation of these intermediates from that of haloaniline products over other metal catalysts. According to the present experimental results and above discussion, we proposed the reaction pathways for the reactions of interest over the Pt/γ-Fe_2O_3 catalyst as shown in Scheme 2. It should be noted that this debromination pathway may also play a role in hydrodebromination during the hydrogenation of BNBs over other metal catalysts.

The evolution of detectable reaction compounds by GC during the hydrogenation courses of *o*-BNB, *m*-BNB and *p*-BNB over Pt/γ-Fe_2O_3 and Pt/C are shown in Figs. 2–7, respectively. Over the Pt/γ-Fe_2O_3 nanocomposite catalyst, the peak area ratio of *o*-BNSB to the internal standard in GC was not more than 6.3 at any stage of the hydrogenation course of *o*-BNB (Fig. 2). While the ratios of *m*-BNSB and *p*-BNSB to the internal standard maintained at a low level of about 1.5 and 2.0, during the whole course of *m*-BNB (Fig. 4) and *p*-BNB (Fig. 6) hydrogenation, respectively. On the contrary, over the Pt/C catalyst, there were obvious build-up processes of the BNSB intermediates during the reaction courses. The highest ratios of *o*-BNSB, *m*-BNSB and *p*-BNSB to the internal standard could reach 23.4 (Fig. 3), 11.5 (Fig. 5) and 13.2 (Fig. 7), respectively. These phenomena indicated that the conversion rates of the BNSB intermediates are much slower than the hydrogenation rates of the BNB substrates over the Pt/C catalyst, and the distinction in the formation rate of BANs over Pt/γ-Fe_2O_3 and Pt/C could be partly attributed to the different catalytic performances over the two catalysts for BNSB intermediates transformation.

In our experiments, during the activation process of the Pt/γ-Fe_2O_3 catalyst with hydrogen at 303 K and atmospheric pressure, a color change from brownish-red to black was observed. As shown in Fig. 8 and Table 5, X-ray diffraction (XRD) measurements on the fresh and activated catalysts revealed that the diffraction pattern of iron oxide particles in the activated catalyst is similar to that in the fresh catalyst, with a very small shift in several diffraction peaks to the lower angle side. Consequently, the Pt/γ-Fe_2O_3 catalyst was partly reduced in the activation process, catalyzed by the Pt nanoclusters, resulting in an increase in the amount of coordinatively unsaturated iron cation species in the activated catalyst's surface.

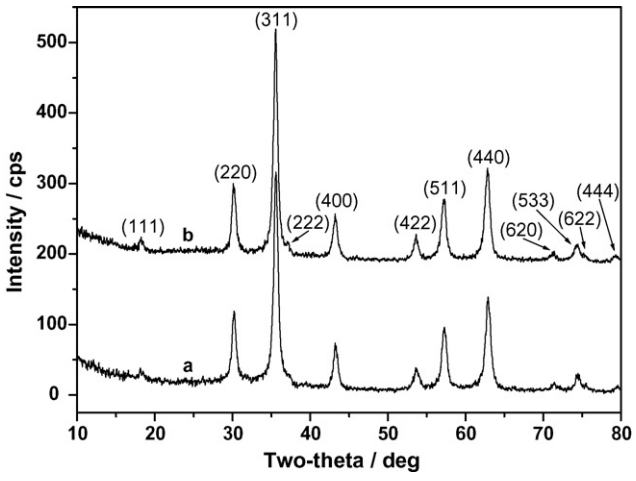

Fig. 8. X-ray diffraction pattern of the fresh Pt/γ-Fe_2O_3 catalyst (a) and the catalyst activated with hydrogen at 303 K and atmospheric pressure (b).

Table 5
X-ray diffraction data of the fresh Pt/γ-Fe_2O_3 catalyst and the activated catalyst

Sample	*d* (0.1 nm) at various *h k l* values						
	(220)	(311)	(400)	(422)	(511)	(440)	(533)
Fresh cat.	2.9531	2.5211	2.0879	1.7049	1.6056	1.4755	1.2734
Activated cat.[a]	2.9569	2.5239	2.0906	1.7049	1.6061	1.4768	1.2740
γ-Fe_2O_3[b]	2.9530	2.5177	2.0886	1.7045	1.6073	1.4758	1.2730
Fe_3O_4[b]	2.9670	2.5320	2.0993	1.7146	1.6158	1.4845	1.2807

[a] *Activation conditions*: Pt/γ-Fe_2O_3, 0.2 g; solvent, 20 ml methanol; temperature, 303 K; hydrogen pressure, 0.1 MPa; time, 30 min.
[b] From Ref. [39].

We have suggested that the vacancies, i.e., the coordinatively unsaturated iron cation species in the catalyst surface may play an important role in the excellent catalytic properties for the hydrogenation of CNB [5]. These species may activate the polar $-NO_2$ and $-NO$ groups in BNB and BNSB, respectively, thereby promote the hydrogenation rates of BNB and BNSB to BAN. On the other hand, the amino group as an electron-donating substitution in the aromatic ring would favor the hydrogenolysis of the carbon–halogen bond in aromatic haloamines [3,40]. The coordination between the $-NH_2$ group in produced BAN molecules and the surface vacancies near to the Pt nanoparticles, which decreases the electron-donating ability of the $-NH_2$ group, may be partly responsible for the excellent selectivity to BAN over the Pt/γ-Fe_2O_3 catalyst. The investigation aiming at revealing the exact catalytic mechanism for the highly selective hydrogenation of halonitrobenzenes to corresponding haloanilines over the Pt/γ-Fe_2O_3 catalyst is under way.

4. Conclusions

The Pt/γ-Fe_2O_3 nanocomposite catalyst exhibited excellent catalytic properties for the selective hydrogenation of *o*-BNB, *m*-BNB and *p*-BNB. The formation rates of *o*-BAN, *m*-BAN and *p*-BAN over the Pt/γ-Fe_2O_3 catalyst were all higher than those over the Pt/C catalyst in methanol at 303 K and 0.1 MPa of hydrogen pressure, due to the high conversion rate of BNSBs over the Pt/γ-Fe_2O_3 nanocomposite catalyst. Under these reaction conditions, the high catalytic selectivities, over 99.7% to *o*-BAN and over 99.8% to *m*-BAN as well as *p*-BAN, could be easily obtained at complete conversion of the substrates. The hydrodebromination of BANs over the nanocomposite catalyst was fully suppressed for the first time. A new debromination pathway in BNBs hydrogenation was revealed over the Pt/γ-Fe_2O_3 catalyst, i.e., through the hydrodebromination of the condensation intermediates, which resulted in trace of AN in the hydrogenation products. Over the Pt/γ-Fe_2O_3 catalyst, elevating hydrogen pressure from 0.1 to 2.0 MPa could not only increase the hydrogenation rates of BNBs by about one order of magnitude, but also improve the selectivities to BANs to a level higher than 99.9%. The Pt/γ-Fe_2O_3 nanocomposite catalyst is of great value for producing BANs with a high purity via highly efficient hydrogenation of BNBs.

Acknowledgements

This work is jointly supported by NSFC (20573005, 50521201, 90206011, 29925308, 20433010), NKBRSF (2006CB806102) from Chinese Ministry of Science and Technology, and RFDP of the Ministry of Education of China.

References

[1] J.O. Morley, J. Phys. Chem. 99 (1995) 1923.
[2] Y. Okazaki, K. Yamashita, H. Ishii, M. Sudo, M. Tsuchitani, J. Appl. Toxicol. 23 (2003) 315.
[3] R. Baltzly, A.P. Phillips, J. Am. Chem. Soc. 68 (1946) 261.
[4] B.J. Zuo, Y. Wang, Q.L. Wang, J.L. Zhang, N.Z. Wu, L.D. Peng, L.L. Gui, X.D. Wang, R.M. Wang, D.P. Yu, J. Catal. 222 (2004) 493.
[5] J.L. Zhang, Y. Wang, H. Ji, Y.G. Wei, N.Z. Wu, B.J. Zuo, Q.L. Wang, J. Catal. 229 (2005) 114.
[6] P. Kapa, T.L. George, C. Apurva, J.G. Michael, W.S. James, R. Oljan, Org. Process Res. Dev. 7 (2003) 723.
[7] F. Ralf, W.K.R.M. Wemer, Helv. Chim. Acta 83 (2000) 1247.
[8] G. Aleem, Y. Jie, A.I. Michael, K. Shekhar, Bioorg. Med. Chem. 11 (2003) 5155.
[9] D.H. Beata, M. Katrien, E. Oliver, K. Laszlo, T. Pal, U.W.M. Bert, R. Zsuzsanna, H. Gyorgy, A.D. Roger, L.F.L. Guy, K. Janez, M. Peter, Tetrahedron 60 (2004) 2283.
[10] H. Steven, U.W.M. Bert, P. Luc, L.F.L. Guy, M. Peter, H. Gyorgy, A.D. Roger, Tetrahedron 61 (2005) 1571.
[11] S. Ian, J.W. Andrew, T. Mary, G.C. Richard, J. Phys. Chem. B 109 (2005) 12636.
[12] G. Aysegul, S. Bekir, T. Muzaffer, J. Appl. Polym. Sci. 98 (2005) 2048.
[13] S. Mohammad, S.M.N. Omar, K.M. Ajax, P.V. Saji, Polyhedron 15 (1996) 1283.
[14] Y.Y. Chen, C. Wang, H.Y. Liu, J.S. Qiu, X.H. Bao, Chem. Commun. 42 (2005) 5298.
[15] X.H. Yan, J.Q. Sun, Y.W. Wang, J.F. Yang, J. Mol. Catal. A 252 (2006) 17.
[16] X.X. Han, R.X. Zhou, G.H. Lai, X.M. Zheng, Catal. Today 93–95 (2004) 433.
[17] X.X. Han, R.X. Zhou, G.H. Lai, X.M. Zheng, React. Kinet. Catal. Lett. 83 (2004) 55.
[18] W.W. Yu, H.F. Liu, J. Mol. Catal. A 243 (2006) 120.
[19] M.H. Liu, B.L. He, H.F. Liu, X.P. Yan, J. Colloid Interf. Sci. 263 (2003) 461.
[20] J. Wiss, A. Zilian, Org. Process Res. Dev. 7 (2003) 1059.
[21] M. Benz, A.M. Draan, R. Prins, Appl. Catal. A 172 (1998) 149.
[22] A.M. Stratz, in: J.R. Kosak (Ed.), Catalysis of Organic Reactions, Dekker, New York, 1984, pp. 335–375.
[23] J.R. Kosak, in: W.H. Jones (Ed.), Catalysis in Organic Syntheses, Academic Press, New York, 1980, pp. 107–117.
[24] W. Pascoe, in: P.N. Rylander (Ed.), Catalysis of Organic Reactions, Dekker, New York, 1988, pp. 121–134.

[25] Y. Wang, J.W. Ren, K. Deng, L.L. Gui, Y.Q. Tang, Chem. Mater. 12 (2000) 1622.
[26] F.Z. Haber, Elektrochemistry 22 (1898) 506.
[27] V. Kratky, M. Kralik, M. Mecarova, M. Stolcova, Appl. Catal. A 235 (2002) 225.
[28] H. Amold, F. Dobert, J. Gaube, in: G. Ertl, H. Knozinger, J. Weitkamp (Eds.), Handbook of Heterogeneous Catalysis, Wiley, New York, 1997, p. 2165.
[29] F. Notheisz, M. Bartok, in: R.A. Sheldon, H.V. Bekkum (Eds.), Fine Chemicals Through Heterogeneous Catalysis, Wiley, New York, 2001, p. 415.
[30] X.L. Yang, H.F. Liu, H. Zhong, J. Mol. Catal. A 147 (1999) 55.
[31] I.A. Ilchenko, A.V. Bulatov, I.E. Uflyand, V.N. Sheinker, Kinet. Catal. 32 (1991) 691.
[32] I.E. Uflyand, I.A. Ilchenko, V.N. Sheinker, A.V. Bulatov, Trans. Metal Chem. 16 (1991) 293.
[33] B. Coq, A. Tijani, F. Figueras, J. Mol. Catal. 68 (1991) 331.
[34] Y. Gao, F. Wang, S. Liao, D. Yu, React. Kinet. Catal. Lett. 64 (1998) 351.
[35] C.V. Rode, M.J. Vaidya, R.V. Chaudhari, Org. Proc. Res. Develop. 3 (1999) 465.
[36] P.N. Rylander, in: J.R. Anderson, M. Boudart (Eds.), Catalysis-Science and Technology, Akademie Verlag, Berlin, 1993, p. 1.
[37] B. Coq, A. Tijani, F. Figueras, J. Mol. Catal. 71 (1992) 317.
[38] S. Galvagno, A. Donato, G. Neri, R. Pietropolo, J. Mol. Catal. 42 (1987) 379.
[39] Powder Diffraction File Hanawalt Search Manual, Inorganic Phase, Sets, 1-42, International Centre for Diffraction Data, Pennsylvania, 1992.
[40] P. Baumeister, H.U. Blaser, W. Scherrer, Stud. Surf. Sci. Catal. 59 (1991) 321.